

# Differentiable Time-Varying IIR Filtering for Real-Time Speech Denoising

Riccardo Rota<sup>1,2,\*\*</sup>, Kiril Ratmanski<sup>1</sup>, Jozef Coldenhoff<sup>1</sup>, Milos Cernak<sup>1</sup>

<sup>1</sup> Logitech Europe S.A., Switzerland

<sup>2</sup> EPFL (École Polytechnique Fédérale de Lausanne), Switzerland

rrota@logitech.com, kratmanski@logitech.com, jcoldenhoff@logitech.com,  
mcernak@logitech.com

## Abstract

We present TVF (Time-Varying Filtering), a low-latency speech enhancement model with 1 million parameters. Combining the interpretability of Digital Signal Processing (DSP) with the adaptability of deep learning, TVF bridges the gap between traditional filtering and modern neural speech modeling. The model utilizes a lightweight neural network backbone to predict the coefficients of a differentiable 35-band IIR filter cascade in real time, allowing it to adapt dynamically to non-stationary noise. Unlike “black-box” deep learning approaches, TVF offers a completely interpretable processing chain, where spectral modifications are explicit and adjustable. We demonstrate the efficacy of this approach on a speech denoising task using the Valentini-Botinhao dataset and compare the results to a static DDSP approach and a fully deep-learning-based solution, showing that TVF achieves effective adaptation to changing noise conditions.

**Index Terms:** DDSP, Time-Varying Filtering, Interpretable Machine Learning, Speech Denoising, Edge AI

## 1. Introduction

While deep learning has transformed audio processing, traditional Digital Signal Processing (DSP) remains vital for low-power applications due to its computational efficiency and interpretability. However, classic DSP struggles to handle dynamic, non-stationary noise without manual tuning. While Differentiable DSP (DDSP), introduced by [1], bridges this gap by embedding DSP blocks into machine learning pipelines, existing methods largely rely on non-causal or offline processing. Fully unconstrained deep learning models excel at waveform matching, but act as “black boxes”, and they frequently introduce unnatural artifacts that degrade perceived audio quality.

To address these limitations, we introduce Time-Varying Filtering (TVF), a lightweight (1M parameters), low-latency system for real-time speech enhancement. TVF employs a neural backbone to dynamically predict the time-varying coefficients of a cascade of 35 second-order IIR filters (biquads) based on the input audio. We overcome the computational bottleneck of deep filter cascades during training by adapting a systolic processing approach into a vectorized tensor formulation for biquad parallelization. Our model is structurally limited to linear time-domain filtering, aiming to prevent artifacts and trade waveform-matching precision for superior perceived audio quality. To the best of our knowledge, TVF represents the first real-time, ML-controlled biquad chain for denoising.

We evaluate our approach against a non-causal static DDSP equalizer [2] and the state-of-the-art ML-based DFNet3 [3]. To

ensure a comparison of architectural efficiency rather than data volume, all models are trained from scratch on the Valentini-Botinhao dataset. Our results demonstrate that TVF effectively adapts to changing noise conditions while preserving the interpretability of a traditional DSP chain.

## 2. Related Work

The Differentiable Digital Signal Processing (DDSP) framework was originally introduced by [1], utilizing a spectral synthesizer to reconstruct and transfer musical instrument timbre. In the domain of audio effects, [2] represents a key contribution, introducing differentiable implementations of Parametric Equalizer (PEQ) and Dynamic Range Compressor. We explicitly adopt their static PEQ formulation as our baseline. These works also laid the foundation for the two most prominent libraries in the field<sup>1,2</sup>. Recent advancements have significantly expanded the DDSP paradigm to target resource-constrained environments, making it highly relevant for real-time edge applications. For instance, [4] proposed an ultra-lightweight differentiable DSP vocoder combining a simple DSP module with a joint acoustic model, achieving high-quality synthesis while surpassing neural baselines in efficiency. Building on this, [5] applied DDSP vocoder refinement to speech enhancement. By driving the vocoder with a compact neural network predicting periodicity, fundamental frequency, and spectral envelope, their framework substantially improved perceptual quality without significant computational overhead.

A significant area of research within this framework is the efficient implementation of IIR filters, typically realized as a cascade of biquad filters [6, 7]. While [8] introduced efficient differentiable time-varying all-pole filters, and recent work by the same authors extended this to biquads [9], these implementations generally target offline applications. To the best of our knowledge, there are no prior examples of real-time, time-varying DSP filtering in this context. The only notable exception is [10], which employs time-varying FIR filters; however, it relies on a feedback loop configuration, limiting its application to specific tasks like echo cancellation. We also mention [11], which proposes a dynamic equalizer similar to this work. However, their model employs a bi-directional GRU, rendering it non-causal and unsuitable for real-time processing.

Regarding speech denoising, we distinguish between large-scale generative models and lightweight real-time models. Large-scale approaches, such as [12, 13] achieve performance close to perfection but are non-causal and computationally prohibitive for on-device deployment. Conversely, lightweight models (ranging from 1M to 10M parameters) are designed

<sup>1</sup><https://github.com/magenta/ddsp>

<sup>2</sup><https://github.com/csteinmetz1/dasp-pytorch>

\*\*indicates the corresponding author.

for real-time operation. Prominent examples include Deep-FilterNet [14, 15, 3], DCCRN [16, 17, 18], and others such as [19, 20, 21, 22]. We also highlight [23], one of the pioneering hybrid DSP/ML approaches, with only 60k parameters. Our proposed model, counting 1.01M parameters, falls into this lightweight category. We select DFNet3 [3] as our benchmark because it has a comparable parameter count (2.31M) and is widely considered the state-of-the-art for real-time denoising.

### 3. Methodology

Our proposed system comprises a machine learning pipeline that controls a chain of 35 cascaded biquad filters. The input audio is segmented into non-overlapping frames of 1024 samples, corresponding to a window of approximately 21 ms at 48 kHz. These frames are processed by two branches, as shown in Figure 1. The machine learning backbone analyzes the signal in the spectral domain and predicts three control parameters: gain ( $g$ ), quality factor ( $q$ ), and center frequency ( $f_0$ ), for each of the 35 biquads per time frame. The cascade of filters then processes the audio frame in the time domain using these time-varying coefficients, and the processed frames are concatenated to reconstruct the final output.

#### 3.1. Machine Learning Backbone

For each frame, the neural backbone first processes the 513-dimensional magnitude spectrum using two 1D convolutional layers (kernel size 5, stride 2). These layers increase the channel depth to 4 while reducing the spectral dimension to 129. The resulting flattened  $4 \times 129$  vector feeds into a 2-layer Gated Recurrent Unit (GRU) with a hidden size of 256. We utilize a GRU because its temporal consistency ensures the predicted biquad parameters vary smoothly over time. This memory mechanism is critical to prevent sudden frequency response discontinuities that could cause audible artifacts (like clicks and pops) when dynamically updating filter coefficients. Finally, a linear projection head with a sigmoid activation maps the GRU output to the 105 filter parameters (3 parameters  $\times$  35 filters). These are scaled to physical ranges: gain  $[-20, 20]$  dB and quality factor  $[0.1, 2.0]$  for all 35 filters, while the frequency range  $[f_{\min}, f_{\max}]$  is specific to each filter. The entire model comprises roughly 1.01 million parameters, with the memory footprint dominated by the GRU weights.

#### 3.2. Time Varying IIR Filter Cascade

The filtering stage employs a differentiable cascade of second-order IIR filters (biquads). For frame  $n$ , the  $k$ -th biquad is defined by the transfer function:

$$H^{(k,n)}(z) = \frac{b_0^{(k,n)} + b_1^{(k,n)}z^{-1} + b_2^{(k,n)}z^{-2}}{1 + a_1^{(k,n)}z^{-1} + a_2^{(k,n)}z^{-2}}, \quad (1)$$

where  $b_i^{(k,n)}$  and  $a_i^{(k,n)}$  are the feedforward and feedback coefficients predicted for the whole frame. We parameterize the filters using three properties: gain ( $g$ ), quality factor ( $q$ ), and center or cutoff frequency ( $f_0$ ). We map these attributes to the filter coefficients  $\mathbf{a}, \mathbf{b}$  using the same formulae as in [2] to obtain the desired frequency response shapes.

Our chain consists of a low frequency suppression filter, 33 band-pass resonant filters and a high frequency roll-off. To constrain the optimization search space, the cutoff frequencies of the two bounding filters are restricted to the intervals [20, 60] Hz and [12000, 22000] Hz, respectively, effectively biasing them to

suppress low-frequency rumble or high-frequency hiss. The remaining 33 filters are distributed to maximize resolution in the speech range. We employ a hybrid spacing strategy: bands are linearly spaced with a bandwidth of approximately 50 Hz up to 1000 Hz to capture the fundamental frequencies of speech, after which the bandwidths progressively widen to cover the higher formants efficiently.

#### 3.3. IIR Filtering Implementation

We implement the time-varying filtering of Equation 1 frame-by-frame using Direct Form I [24, pp. 393–400]:

$$w^{(k)}[t] = \sum_{i=0}^2 b_i^{(k,n)} x^{(k)}[t-i], \quad (2)$$

$$y^{(k)}[t] = w^{(k)}[t] - \sum_{i=1}^2 a_i^{(k,n)} y^{(k)}[t-i], \quad (3)$$

where  $x^{(k)}[t]$ ,  $y^{(k)}[t]$ , and  $w^{(k)}[t]$  are the  $t$ -th time sample of the  $n$ -th frame of the input, output, and intermediate state for the  $k$ -th filter, respectively. Note that the input to the first filter is the original audio ( $x^{(0)}[t] = x[t]$ ), and subsequent filters take the previous output ( $x^{(k)}[t] = y^{(k-1)}[t]$ ). We compute Equation 3 using the recursive implementation of an all-poles filter from [8]<sup>3</sup>. We pass the last 2 samples of both  $x^{(k)}$  and  $y^{(k)}$  to the next frame to handle the state correctly.

A naive sequential computation of the  $K$ -biquad cascade over  $N$  frames requires a nested loop of depth  $K \times N$ . To optimize this, we adapt the systolic processing approach [25] into a vectorized tensor formulation, reducing the depth to  $N + K - 1$ . We construct time-shifted coefficient matrices  $\tilde{\mathbf{A}}, \tilde{\mathbf{B}} \in \mathbb{R}^{K \times (N+K-1) \times 3}$ . For a generic matrix  $\tilde{\mathbf{C}} \in \{\tilde{\mathbf{A}}, \tilde{\mathbf{B}}\}$ , the parameter sequence  $\mathbf{c}_n^{(k)} \in \mathbb{R}^3$  of the  $k$ -th filter is shifted forward by  $k$  zero-padded steps. Concurrently, we define a parallel input vector  $\mathbf{X}_n \in \mathbb{R}^K$ :

$$\tilde{\mathbf{C}} = \begin{bmatrix} \mathbf{c}_0^{(0)} & \mathbf{c}_1^{(0)} & \cdots & \mathbf{c}_{N-1}^{(0)} & \mathbf{0} & \cdots \\ \vdots & \ddots & \ddots & \ddots & \ddots & \ddots \\ \cdots & \mathbf{0} & \mathbf{c}_0^{(K-1)} & \mathbf{c}_1^{(K-1)} & \cdots & \mathbf{c}_{N-1}^{(K-1)} \end{bmatrix}, \quad (4)$$

$$\mathbf{X}_n = [\mathbf{x}_n, \mathbf{y}_{n-1}^{(0)}, \dots, \mathbf{y}_{n-1}^{(K-2)}]^\top.$$

At any execution step  $n \in [0, N+K-2]$ , the  $n$ -th column slices of  $\tilde{\mathbf{A}}$  and  $\tilde{\mathbf{B}}$  align the exact coefficients required to process all  $K$  filters simultaneously. By feeding these slices and  $\mathbf{X}_n$  into Equations 2 and 3, we implicitly create a 1-sample delay chain that replaces the  $K \times N$  deep recurrences with efficient parallel matrix operations. While this systolic vectorization drastically accelerates training, it introduces a 35-frame algorithmic latency. Consequently, at inference time, we use the standard serial implementation to maintain a low latency of 21 ms.

#### 3.4. Weights Initialization

To improve training stability, we initialize the final linear layer’s gain parameters near 0 dB (with minor noise) so the model begins in an “all-pass” state. Standard random initialization often caused overly aggressive initial frequency responses, trapping the model in poor local minima that suppressed the entire signal or wasting dozens of epochs just learning to pass the signal through. Our approach prevents these pitfalls and significantly accelerates convergence.

<sup>3</sup><https://github.com/ewan-xu/torchlpc>

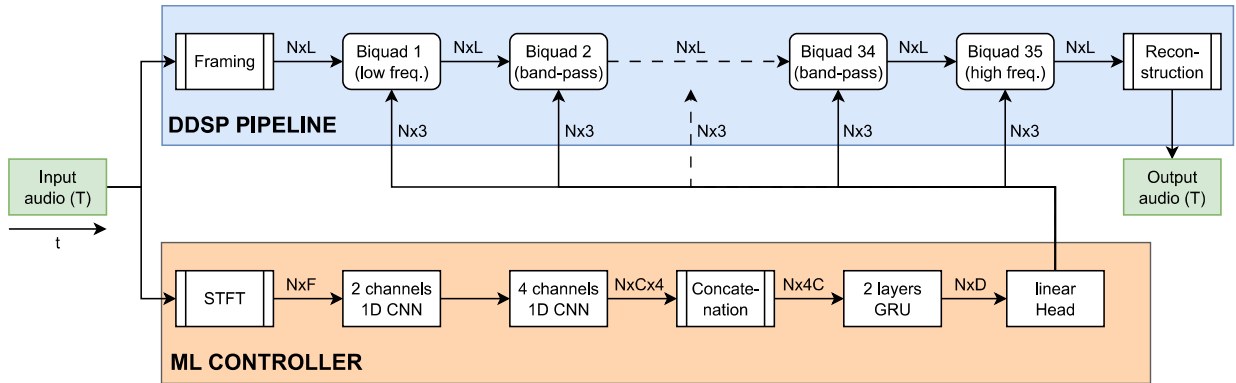


Figure 1: *Model architecture: Here  $T$  is the total number of samples,  $N$  is the number of frames,  $L = 1024$  is the frame length,  $F = 513$  is the number of frequency bins,  $C = 129$  is the number of features per channel after the two convolutions,  $D = 256$  is the hidden and output dimension of the GRU.*

### 3.5. The Static PEQ Baseline

To isolate the benefit of time-varying control, we compare against the PEQ implementation by [2]<sup>1</sup>, extended to 35 bands. We employ the same 1.01M parameter backbone used by TVF, but apply global average pooling after the GRU. This grants the baseline access to the full signal context (non-causal processing) but restricts it to predicting a single set of parameters applied uniformly to the entire clip.

## 4. Experiments

We evaluate our TVF model on a speech denoising task, comparing it against the static PEQ [2] described in the previous section and the DeepFilterNet3 (DFNet3) model [3].

### 4.1. Dataset

We train all three models using the 56-speaker Valentini-Botinhao noisy speech dataset [26]. While relatively small compared to modern large-scale corpora, it remains a standard benchmark for comparing models under data constraints and evaluating the architecture rather than the volume of data. The dataset contains 19 hours of clean speech mixed with various noise samples. We reserve files from 12 speakers for validation and use the remaining 44 speakers as the training set.

We obtain pure noise tracks by computing the difference between the clean and noisy pairs, subsequently using them for data augmentation. We follow the data augmentation strategy of DFNet, which consists of dynamically mixing random speech and noise files at each training iteration with a signal-to-noise ratio (SNR) sampled from the set  $\{-5, 0, 5, 10, 20, 40, 100\}$  dB. We explicitly include the 100 dB samples to teach the models to handle noise-free audio effectively without introducing unwanted distortion. Finally, we evaluate performance on the standard test set, which consists of 824 files recorded by two distinct speakers, paired with their clean references.

### 4.2. Training Setup

Because the original DFNet3 model was trained on a significantly larger dataset, we retrained it from scratch to ensure a fair baseline comparison. Consequently, we anticipate lower performance metrics than those reported by the original authors on this specific test set. We adhered to the default hyperparam-

eters provided in the official source code<sup>4</sup>, training with a batch size of 64 for 100 epochs. The best-performing model checkpoint was restored at epoch 67.

For the PEQ and TVF models, we optimize a loss function comprising a multi-scale logarithmic spectral distance and a time-domain Mean Squared Error term, scaled by a factor of  $5 \times 10^4$ . We use a batch size of 64 and train for 100 epochs. Optimization is performed using Adam [27, 28] with a fixed learning rate of  $10^{-3}$  and standard PyTorch parameters ( $\beta_1 = 0.9$ ,  $\beta_2 = 0.999$ ,  $\epsilon = 10^{-8}$ ). The best validation losses were achieved at epochs 72 and 63 for PEQ and TVF, respectively.

### 4.3. Evaluation Metrics

We evaluate the enhanced audio using eight metrics. For reference-based fidelity, we measure perceptual speech quality using PESQ [29] and the wideband-optimized POLQA [30] (both scaled 1–5). Intelligibility is predicted via eSTOI [31] (scaled 0–1), while time-domain distortion is evaluated using SI-SDR [32] (in dB). Spectral accuracy is quantified by the Log-Spectral Distance (LSD), calculated using 256-sample frames with a 128-sample overlap. To assess perceived quality without a clean reference, we utilize SIGMOS [33], an improved DNSMOS estimator [34]. It provides three scores scaled 1–5: MOS-Signal (speech quality), MOS-Noise (background noise suppression), and MOS-Overall (combined quality). For all metrics except LSD, higher scores indicate better performance.

## 5. Results

We evaluate the performance of the three models using the metrics defined in the previous section. Table 1 presents the mean values and standard deviations obtained across the 824 files in the test set. The first column reports the metrics computed on the unprocessed input signal for reference. It is important to contextualize the performance of the DFNet3 baseline. In our experiments, it achieves a PESQ of 2.13, lower than the score of 3.17 reported by the original authors [3]. This difference is expected, as the original model was trained on thousands of hours of speech, whereas we trained it on the significantly smaller Valentini-Botinhao dataset to ensure a fair comparison of the architectures under identical data constraints.

<sup>4</sup><https://github.com/Rikorose/DeepFilterNet>

Table 1: Mean and standard deviation of objective metrics and model complexity.

Metric	Input Signal	Static PEQ	DFNet3	TVF (Ours)
PESQ ( $\uparrow$ )	1.97 $\pm$ 0.75	2.13 $\pm$ 0.71	2.12 $\pm$ 0.63	<b>2.14</b> $\pm$ 0.62
POLQA ( $\uparrow$ )	3.27 $\pm$ 0.85	3.44 $\pm$ 0.80	3.28 $\pm$ 0.94	<b>3.50</b> $\pm$ 0.94
eSTOI ( $\uparrow$ )	0.79 $\pm$ 0.15	0.78 $\pm$ 0.15	<b>0.80</b> $\pm$ 0.14	0.79 $\pm$ 0.14
LSD ( $\downarrow$ )	3.39 $\pm$ 1.67	2.13 $\pm$ 1.26	<b>1.40</b> $\pm$ 0.81	1.97 $\pm$ 0.99
SI-SDR ( $\uparrow$ )	8.39 $\pm$ 5.62	10.82 $\pm$ 4.32	<b>14.58</b> $\pm$ 3.16	13.71 $\pm$ 4.03
MOS-Noise ( $\uparrow$ )	2.29 $\pm$ 0.89	2.41 $\pm$ 0.87	2.90 $\pm$ 0.67	<b>3.61</b> $\pm$ 0.70
MOS-Signal ( $\uparrow$ )	3.17 $\pm$ 0.49	<b>3.19</b> $\pm$ 0.49	3.02 $\pm$ 0.66	2.95 $\pm$ 0.63
MOS-Overall ( $\uparrow$ )	2.46 $\pm$ 0.64	2.52 $\pm$ 0.58	2.57 $\pm$ 0.62	<b>2.64</b> $\pm$ 0.53
Parameters	–	1.01 M	2.31 M	1.01 M

### 5.1. Objective Evaluation

The first five rows of Table 1 compare the processed audio with the clean reference. We observe that TVF leverages its adaptability to outperform the static PEQ baseline, despite the static PEQ having the advantage of non-causality. Compared to the input signal, TVF improves the average SI-SDR by 5.32 dB and demonstrates performance comparable to DFNet3. TVF performs even better than DFNet3 on PESQ and POLQA metrics. The eSTOI metric remains consistent with the input score; this is expected given the high initial intelligibility of the Valentini-Botinhao test set, indicating that our model successfully preserves speech content while suppressing noise.

### 5.2. Perceptual Quality Assessment

Reference-free SIGMOS metrics (Table 1, rows 6–8) show that despite a slight increase in signal distortion, our model achieves superior noise reduction (MOS-Noise), yielding the highest MOS-Overall score. Importantly, this aggressive denoising profile is a tunable feature rather than a fixed constraint; the trade-off between noise suppression and signal preservation can be controlled by adjusting the weight of the time-domain loss term.

### 5.3. Spectral Adaptation Analysis

We further analyze the behavior of TVF by plotting its frequency response over time (Figure 2). We can observe that the model effectively attenuates all noise in the first 0.5 seconds of the example, where no speech is present, by applying a -40 dB gain to the entire spectrum. When speech starts, the filters adapt by setting a 0 dB gain in the frequencies where speech is detected and applying negative gain to the rest of the spectrum. We also observe that the transition is always continuous, thanks to the GRU features changing smoothly. This avoids artifacts in the output that would be present if biquad coefficients changed too suddenly. By looking at the output spectrogram, we note that the noise has been removed, and the speech is mostly preserved, despite some degradation in the high frequencies. This confirms the numerical values obtained with the MOS metrics.

## 6. Conclusion and Future Work

While TVF and DFNet both target real-time speech enhancement, they rely on fundamentally different paradigms. DFNet operates as a deep STFT-domain masker, predicting complex

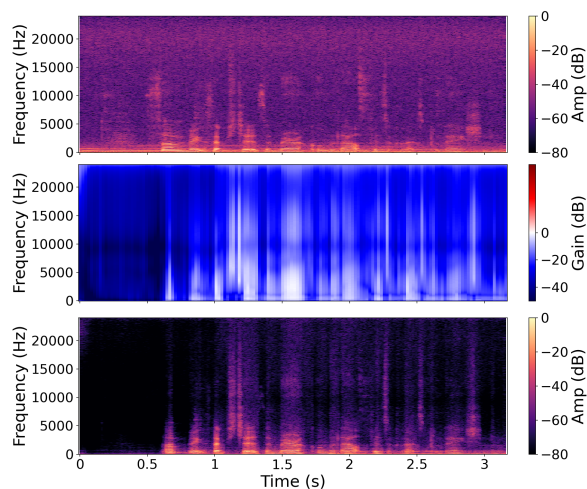


Figure 2: Analysis of the filtering on a track with non-stationary background noise. From top to bottom: noisy input spectrogram, adaptive frequency response of TVF, denoised output.

weights to reconstruct phase and periodicity. This unconstrained, “black box” approach excels on waveform-matching metrics like SI-SDR and LSD. In contrast, TVF applies linear time-domain filtering by mapping neural outputs to physically constrained IIR parameters. This strict inductive bias acts as a natural regularizer. While it cannot perform the non-linear phase reconstruction typical of complex masks, this structural constraint prevents unnatural neural synthesis artifacts, allowing the model to excel in data-constrained scenarios. Consequently, TVF achieves strong results on human perceptual metrics like PESQ, POLQA, and SIGMOS. Ultimately, TVF trades the advantages of complex masking for strict interpretability, stability, and artifact-free linear processing.

This work serves as a proof of concept, demonstrating that a lightweight neural network can effectively control a biquad chain for real-time speech enhancement. Future work will involve training TVF on significantly larger-scale datasets to provide a more rigorous comparison against state-of-the-art models. Additionally, we plan to optimize the model architecture and the loss function to better refine the trade-off between noise suppression and speech preservation, alongside exploring extensions to support stereo and multi-channel audio processing.

## 7. AI Disclosure

The authors acknowledge the use of Google Gemini for the purpose of copyediting and polishing the English language in this manuscript.

## 8. References

- [1] J. Engel, L. H. Hantrakul, C. Gu, and A. Roberts, "Ddsp: Differentiable digital signal processing," in *International Conference on Learning Representations*, 2020. [Online]. Available: <https://openreview.net/forum?id=B1x1ma4tDr>
- [2] C. J. Steinmetz, N. J. Bryan, and J. D. Reiss, "Style Transfer of Audio Effects with Differentiable Signal Processing," *Journal of the Audio Engineering Society*, vol. 70, no. 9, pp. 708–721, Nov. 2022. [Online]. Available: <https://www.aes.org/e-lib/browse.cfm?elib=21883>
- [3] H. Schröter, T. Rosenkranz, A. N. Escalante-B., and A. Maier, "DeepFilterNet: Perceptually Motivated Real-Time Speech Enhancement," in *INTERSPEECH*, 2023.
- [4] P. Agrawal, T. Koehler, Z. Xiu, P. Serai, and Q. He, "Ultra-Lightweight Neural Differential DSP Vocoder for High Quality Speech Synthesis," in *ICASSP 2024 - 2024 IEEE International Conference on Acoustics, Speech and Signal Processing (ICASSP)*. Seoul, Korea, Republic of: IEEE, Apr. 2024, pp. 10066–10070. [Online]. Available: <https://ieeexplore.ieee.org/document/10447948/>
- [5] H. R. Guimarães, K. Tan, J. Azcarreta, J. Alvarez, P. Agrawal, A. Pandey, and B. Xu, "Improving Resource-Efficient Speech Enhancement via Neural Differentiable DSP Vocoder Refinement," 2025. [Online]. Available: <https://arxiv.org/abs/2508.14709>
- [6] J. T. Colonel, C. J. Steinmetz, M. Michelen, and J. D. Reiss, "Direct Design of Biquad Filter Cascades with Deep Learning by Sampling Random Polynomials," in *ICASSP 2022 - 2022 IEEE International Conference on Acoustics, Speech and Signal Processing (ICASSP)*. Singapore, Singapore: IEEE, May 2022, pp. 3104–3108. [Online]. Available: <https://ieeexplore.ieee.org/document/9747660/>
- [7] B. Kuznetsov, J. D. Parker, and F. Esqueda, "Differentiable IIR Filters for Machine Learning Applications," in *Proceedings of the 23rd International Conference on Digital Audio Effects (DAFx2020)*, Vienna, Austria, Sep. 2020, pp. 297–303.
- [8] C.-Y. Yu, C. Mitcheltree, A. Carson, S. Bilbao, J. D. Reiss, and G. Fazekas, "Differentiable All-pole Filters for Time-varying Audio Systems," in *International Conference on Digital Audio Effects (DAFx)*, 2024, pp. 345–352.
- [9] C.-Y. Yu and G. Fazekas, "Accelerating Automatic Differentiation of Direct Form Digital Filters," Nov. 2025, arXiv:2511.14390. [Online]. Available: <http://arxiv.org/abs/2511.14390>
- [10] J. Casebeer, N. J. Bryan, and P. Smaragdis, "Meta-AF: Meta-Learning for Adaptive Filters," *IEEE/ACM Transactions on Audio, Speech, and Language Processing*, vol. 31, pp. 355–370, 2023. [Online]. Available: <https://ieeexplore.ieee.org/document/9961879/>
- [11] P. Sarkar and P. Lindborg, "Diff-DEQ: Differentiable Dynamic Equalization for Studio-Quality Speech Processing," in *2025 33rd European Signal Processing Conference (EUSIPCO)*. Palermo, Italy: IEEE, Sep. 2025, pp. 511–515. [Online]. Available: <https://ieeexplore.ieee.org/document/11226258/>
- [12] B. Shi, A. Tjandra, J. Hoffman, H. Wang, Y.-C. Wu, L. Gao, J. Richter, M. Le, A. Vyas, S. Chen, C. Feichtenhofer, P. Dollár, W.-N. Hsu, and A. Lee, "SAM Audio: Segment Anything in Audio," Dec. 2025, arXiv:2512.18099. [Online]. Available: <http://arxiv.org/abs/2512.18099>
- [13] J. Richter, S. Welker, J.-M. Lemerrier, B. Lay, and T. Gerkmann, "Speech Enhancement and Dereverberation With Diffusion-Based Generative Models," *IEEE/ACM Transactions on Audio, Speech, and Language Processing*, vol. 31, pp. 2351–2364, 2023. [Online]. Available: <https://ieeexplore.ieee.org/document/10149431/>
- [14] H. Schröter, A. N. Escalante-B, T. Rosenkranz, and A. Maier, "Deepfilternet: A Low Complexity Speech Enhancement Framework for Full-Band Audio Based On Deep Filtering," in *ICASSP 2022 - 2022 IEEE International Conference on Acoustics, Speech and Signal Processing (ICASSP)*. Singapore, Singapore: IEEE, May 2022, pp. 7407–7411. [Online]. Available: <https://ieeexplore.ieee.org/document/9747055/>
- [15] H. Schröter, A. Maier, A. Escalante-B, and T. Rosenkranz, "Deepfilternet2: Towards Real-Time Speech Enhancement on Embedded Devices for Full-Band Audio," in *2022 International Workshop on Acoustic Signal Enhancement (IWAENC)*. Bamberg, Germany: IEEE, Sep. 2022, pp. 1–5. [Online]. Available: <https://ieeexplore.ieee.org/document/9914782/>
- [16] Y. Hu, Y. Liu, S. Lv, M. Xing, S. Zhang, Y. Fu, J. Wu, B. Zhang, and L. Xie, "DCCRN: Deep Complex Convolution Recurrent Network for Phase-Aware Speech Enhancement," in *Interspeech 2020*. ISCA, Oct. 2020, pp. 2472–2476. [Online]. Available: [https://www.isca-archive.org/interspeech\\_2020/hu20g\\_interspeech.html](https://www.isca-archive.org/interspeech_2020/hu20g_interspeech.html)
- [17] S. Lv, Y. Fu, M. Xing, J. Sun, L. Xie, J. Huang, Y. Wang, and T. Yu, "S-DCCRN: Super Wide Band DCCRN with Learnable Complex Feature for Speech Enhancement," in *ICASSP 2022 - 2022 IEEE International Conference on Acoustics, Speech and Signal Processing (ICASSP)*. Singapore, Singapore: IEEE, May 2022, pp. 7767–7771. [Online]. Available: <https://ieeexplore.ieee.org/document/9747029/>
- [18] S. Lv, Y. Hu, S. Zhang, and L. Xie, "DCCRN+: Channel-Wise Subband DCCRN with SNR Estimation for Speech Enhancement," in *Interspeech 2021*. ISCA, Aug. 2021, pp. 2816–2820. [Online]. Available: [https://www.isca-archive.org/interspeech\\_2021/lv21\\_interspeech.html](https://www.isca-archive.org/interspeech_2021/lv21_interspeech.html)
- [19] G. Yu, Y. Guan, W. Meng, C. Zheng, H. Wang, and Y. Wang, "DMF-Net: A decoupling-style multi-band fusion model for full-band speech enhancement," in *2022 Asia-Pacific Signal and Information Processing Association Annual Summit and Conference (APSIPA ASC)*. Chiang Mai, Thailand: IEEE, Nov. 2022, pp. 1382–1387. [Online]. Available: <https://ieeexplore.ieee.org/document/9980012/>
- [20] S. Braun, H. Gamper, C. K. Reddy, and I. Tashev, "Towards Efficient Models for Real-Time Deep Noise Suppression," in *ICASSP 2021 - 2021 IEEE International Conference on Acoustics, Speech and Signal Processing (ICASSP)*. Toronto, ON, Canada: IEEE, Jun. 2021, pp. 656–660. [Online]. Available: <https://ieeexplore.ieee.org/document/9413580/>
- [21] H. Schröter, T. Rosenkranz, A. N. Escalante-B, M. Aubreville, and A. Maier, "CLCNET: Deep Learning-Based Noise Reduction for Hearing aids using Complex Linear Coding," in *ICASSP 2020 - 2020 IEEE International Conference on Acoustics, Speech and Signal Processing (ICASSP)*. Barcelona, Spain: IEEE, May 2020, pp. 6949–6953. [Online]. Available: <https://ieeexplore.ieee.org/document/9053563/>
- [22] J. Chen, Z. Wang, D. Tuo, Z. Wu, S. Kang, and H. Meng, "FullSubNet+: Channel Attention Fullsubnet with Complex Spectrograms for Speech Enhancement," in *ICASSP 2022 - 2022 IEEE International Conference on Acoustics, Speech and Signal Processing (ICASSP)*. Singapore, Singapore: IEEE, May 2022, pp. 7857–7861. [Online]. Available: <https://ieeexplore.ieee.org/document/9747888/>
- [23] J.-M. Valin, "A Hybrid DSP/Deep Learning Approach to Real-Time Full-Band Speech Enhancement," in *2018 IEEE 20th International Workshop on Multimedia Signal Processing (MMSp)*. Vancouver, BC: IEEE, Aug. 2018, pp. 1–5. [Online]. Available: <https://ieeexplore.ieee.org/document/8547084/>
- [24] A. V. Oppenheim and R. W. Schaffer, *Discrete-Time Signal Processing*, 3rd ed. Pearson Education, 2013, pearson New International Edition.
- [25] Kung, H. T., "Why systolic architectures?" *Computer*, vol. 15, no. 1, pp. 37–46, Jan. 1982. [Online]. Available: <http://ieeexplore.ieee.org/document/1653825/>

- [26] C. Valentini-Botinhao, “Noisy speech database for training speech enhancement algorithms and TTS models,” 2017. [Online]. Available: <https://datashare.ed.ac.uk/handle/10283/2791>
- [27] D. P. Kingma and J. Ba, “Adam: A Method for Stochastic Optimization,” in *3rd International Conference on Learning Representations (ICLR)*, San Diego, CA, USA, 2015.
- [28] A. Paszke, S. Gross, F. Massa, A. Lerer, J. Bradbury, G. Chanan, T. Killeen, Z. Lin, N. Gimelshein, L. Antiga, A. Desmaison, A. Köpf, E. Yang, Z. DeVito, M. Raison, A. Tejani, S. Chilamkurthy, B. Steiner, L. Fang, J. Bai, and S. Chintala, “PyTorch: An Imperative Style, High-Performance Deep Learning Library,” in *Advances in Neural Information Processing Systems 32*. Curran Associates, Inc., 2019, pp. 8024–8035.
- [29] A. Rix, J. Beerends, M. Hollier, and A. Hekstra, “Perceptual evaluation of speech quality (PESQ)-a new method for speech quality assessment of telephone networks and codecs,” in *2001 IEEE International Conference on Acoustics, Speech, and Signal Processing. Proceedings (Cat. No.01CH37221)*, vol. 2. Salt Lake City, UT, USA: IEEE, 2001, pp. 749–752. [Online]. Available: <http://ieeexplore.ieee.org/document/941023/>
- [30] ITU-T, “Recommendation P.863: Perceptual objective listening quality assessment,” Geneva, Switzerland, 2018.
- [31] J. Jensen and C. H. Taal, “An Algorithm for Predicting the Intelligibility of Speech Masked by Modulated Noise Maskers,” *IEEE/ACM Transactions on Audio, Speech, and Language Processing*, vol. 24, no. 11, pp. 2009–2022, Nov. 2016. [Online]. Available: <https://ieeexplore.ieee.org/document/7539284/>
- [32] J. L. Roux, S. Wisdom, H. Erdogan, and J. R. Hershey, “SDR – Half-baked or Well Done?” in *ICASSP 2019 - 2019 IEEE International Conference on Acoustics, Speech and Signal Processing (ICASSP)*. Brighton, UK: IEEE, May 2019, pp. 626–630. [Online]. Available: <https://ieeexplore.ieee.org/document/8683855/>
- [33] N.-C. Ristea, A. Saabas, R. Cutler, B. Naderi, S. Braun, and S. Branets, “ICASSP 2024 Speech Signal Improvement Challenge,” in *2024 IEEE International Conference on Acoustics, Speech, and Signal Processing Workshops (ICASSPW)*. Seoul, Korea, Republic of: IEEE, Apr. 2024, pp. 15–16. [Online]. Available: <https://ieeexplore.ieee.org/document/10626457/>
- [34] C. K. A. Reddy, V. Gopal, and R. Cutler, “Dnsmos: A Non-Intrusive Perceptual Objective Speech Quality Metric to Evaluate Noise Suppressors,” in *ICASSP 2021 - 2021 IEEE International Conference on Acoustics, Speech and Signal Processing (ICASSP)*. Toronto, ON, Canada: IEEE, Jun. 2021, pp. 6493–6497. [Online]. Available: <https://ieeexplore.ieee.org/document/9414878/>